THE INFLUENCE OF ALLEY CROPPING SYSTEMS ON SOIL WATER DYNAMICS AND SOIL EROSION IN A CHANGING CLIMATE

Progress report *R-1334* *March 2012*

THE INFLUENCE OF ALLEY CROPPING SYSTEMS ON SOIL WATER DYNAMICS AND SOIL EROSION IN A CHANGING CLIMATE

Progress report

Ouranos-ICAR- PACC-26-Biodiversity Project

By

Alain N. ROUSSEAU
Dennis W. HALLEMA
Silvio J. GUMIERE
Gwenael CARRER
Maxime FOSSEY

Institut national de la recherche scientifique
490, rue de la Couronne
Québec (Québec) G1K 9A9

Report R-1334

March 2012

ISBN : 978-2-89146-752-0

Progress report project PACC-26
The influence of alley cropping systems on soil water dynamics and soil erosion in a changing climate
INRS-ETE

Alain N. Rousseau[1], Dennis W. Hallema[1], Silvio J. Gumiere[2],
Gwenael Carrer[1] and Maxime Fossey[1]

[1] *Institut National de la Recherche Scientifique, Centre Eau, Terre et Environnement (INRS-ETE), 490 rue de la Couronne, Quebec, QC G1K 9A9, Canada*

[2] *Université Laval, Département des Sols et de Génie Agroalimentaire, 2480 boulevard Hochelaga, Quebec, QC G1V 0A6, Canada*

March 8, 2012

Contents

Chapter 1

Introduction

1.1 Project overview

The Ouranos-ICAR biodiversity project PACC-26[1] led by Alain Olivier (Université Laval) aims to contribute to the understanding of the influence of alley cropping systems on hydrology and soil erosion by means of physically-based modelling. Alley cropping is an agroforestry practice, mostly applied in regions with a temperate climate, whereby trees are planted at wide spacings, creating alleyways within which companion crops are grown (Garrett et al., 2011). The implementation of alley cropping systems influences the local thermal energy balance and water balance, leading to changes in airflow in and around the plant canopy (Wilson and Shaw, 1977), different solar irradiance, and changes in the amount of evapotranspiration and thermal energy that is stored. Other examples of differences with respect to monoculture practiced in most agricultural regions involve water uptake by plant roots and sediment transport and trapping in and around alley cropping systems (Plamboeck et al., 1999; Gumiere et al., 2010a; Gumiere and Rousseau, 2011). In the light of changing environmental conditions caused by a shift in the local climate, the objective of the current project is to:

> Quantify and evaluate the influence of alley cropping systems on soil water dynamics and soil erosion by surface runoff.

Soil water dynamics and soil erosion by surface runoff depend in varying degrees on:

- Plant species (e.g. distribution of the root system, stage of growth);
- Meteorological variables (e.g. temperature, solar irradiance, precipitation and wind);
- Upstream contributing area in terms of runoff;
- Soil characteristics (e.g. texture, soil type, porosity).

Meteorological variables result from the interaction between the thermal energy balance at the soil surface (net radiation, latent and sensible heat flux) and the atmospherical water balance (athmospheric density, vapor pressure deficit; Penman, 1948; Monteith, 1981). Depending on the local conditions of the environment in which alley cropping is practiced, we can expect that alley cropping systems influence local meteorological variables as well as the water distribution in the soil and at the soil surface. As such, it is possible that alley cropping provides a certain degree of resilience to drought and increased rainfall intensity expected for southern Quebec, Canada (Mailhot et al., 2007).

[1] PACC=Plan d'Action sur les Changements Climatiques

Figure 1.1: Selected alley cropping site near St. Paulin in Mauricie, QC. Tree rows are planted at a 15 m spacing, and are not continuous in the row direction (photograph made on May 5th, 2011).

1.2 Approach and progress

In the course of 2011 we have developed an approach in order to quantify and evaluate the influence of alley cropping systems on soil water dynamics and on soil erosion by surface runoff. The approach revolves around three principal themes, which include sampling and computational modelling of:

1. Soil water dynamics;
2. Soil erosion by water;
3. The behaviour of the two processes above under different climate conditions.

We will elaborate on these three themes in the sections that follow.

1.2.1 Modelling soil water dynamics

We have selected HYDRUS 2D/3D as the modelling environment in which we will develop a soil water distribution model of the alley cropping system. HYDRUS traces its roots to the SWMS_2D model (Šimůnek et al., 1992; based on Van Genuchten, 1987), which later evolved into a software package for simulating two- and three-dimensional movement of water, heat and solutes in variably saturated media (Šimůnek et al., 2011; Šejna et al., 2011). More particularly, the physically-based and conceptual equations that represent hydrological processes within the model allow for simulating:

- Precipitation, infiltration, groundwater flow, throughflow and seepage using Richards equation (Richards, 1931);

- Transpiration throught root uptake by vegetation using Feddes linear water stress response function (Feddes et al., 1978, 2001);
- Evaporation from the soil surface and actual transpiration (together called evapotranspiration) using the Penman-Monteith equation (Penman, 1948; Monteith, 1981).

The governing equations mentioned for the aforementioned processes are widely accepted by environmental researchers and used in many distributed and lumped physically-based models that have been developed over the last decades. The HYDRUS 2D/3D permits simulations on a time scale anywhere between event-based and continuous-time, and on a spatially distributed scale between a soil column and field sized surface. In the current phase of the project we are mainly interested in soil water distribution at the plot scale, as this is the scale at which we can observe changes in local variables that play a role on the scale at which intervention takes place: the field scale.

In order to parameterise and calibrate the individual models, we have conducted field work during the extended growing season (May-November) of 2011 intended to gather weather data and data on soil moisture content. For our 2011 field campaign, we selected the St. Paulin experimental alley cropping site in southern Quebec, Canada, which has been an research site in the studies of Alain Olivier (professor at the Phytology Department of Université Laval), and which is also the site on which Alain Paquette and Susy Domenicano (CEF, UdeM) concentrate their research on C-fixation and photosynthesis growth of the red oak and hybrid poplar that form the tree rows of system.

During the 2011 field campaign, the meteorological variables air pressure, relative humidity, rainfall, temperature, photosynthetically active radiation (PAR), wind speed and direction, were monitored using a portable weather station. Soil moisture data are important in establishing the soil water rentention curve, which we need to estimate soil water storage, water supply to plants and soil aggregate stability. They were obtained using 45 frequency domain reflectometry (FDR) sensors implanted in the soil along a 35 m transect perpendicular to the tree rows of the alley cropping system. The field work season of 2011 was completed succesfully and yielded high quality datasets. Weather data have been analysed, and we are currently in the process of analysing the soil moisture data and preparing a hydrological model for soil water dynamics. As of today, this part of the project is slightly ahead of schedule.

1.2.2 Modelling water erosion

Anthropogenic influence due to intensive agriculture is often the cause of accelerated erosion with ablation rates higher than the rates of the processes that to the formation of soil (pedogenesis). Water erosion can be observed all over the world, sometimes more intense than other. Modelling water erosion potentially provides useful information for the implementation of Beneficial Management Practices (BMPs) on agricultural watersheds, which may enable us to better conserve soil resources and reduce sediment transport toward streams. The implementation of structural BMPs such as alley cropping systems, farm forestry can modify flow paths and sediment connectivity in an agricultural watershed (Gumiere et al., 2010a). It is therefore of great importance that the erosion model applied in this context is able to take into account the influence of structural BMPs on erosion and runoff at the watershed scale (drainage area $<250\ km^2$) and subbasin scale (250-2500 km^2).

For this project we propose to use the water erosion model MHYDAS-Erosion (Gumiere et al., 2010b). MHYDAS-Erosion is an event-based physically-based distributed model that simulates linear erosion in agricultural watersheds. MHYDAS-Erosion is based on a spatial subdivision into *surface units* and segmentation of the drainage network into *channel sections*. Each surface unit is connected on the downstream end either to a surface unit (if there is one) or to a channel section. The boundaries of spatial units are recorded as vector shapes, so that they can take virtually any form. The model framework thus allows for adding spatial discontinuities and a time-variable (dynamic) land use which is characteristic of the agricultural landscape. For example, Gumiere et al. (2010a) demonstrated that MHYDAS-Erosion can take into account spatial discontinuities in the form of

BMPs using distributed descriptions of these features. We expect that, although the model was developed to simulate erosion at the watershed scale, it can also be applied at the field scale.

Since MHYDAS-Erosion has been developed according to the principle of parsimony, the number of parameters is limited. The main input variables are: rainfall intensity (5 min time step), soil map, land use map and land register. As part of this project we will use MHYDAS-Erosion to simulate soil loss and subsequently evaluate the influence of alley cropping systems on soil water dynamics and soil erosion by surface runoff.

1.2.3 Modelling soil water dynamics for a changing climate

After calibrating the soil water distribution model using field data, we will simulate the influence of different vegetation species and tree row distance on soil water dynamics for future climate scenarios. The initial conditions required for simulating soil water patterns with the soil water distribution model can be estimated from historical meteorological data and climate forecasts. The climate simulations available from Ouranos (which is the Quebec Consortium on Regional Climatology and Adaptation to Climate Change) will provide the necessary meteorological variables, such as rainfall, air temperature, latent and sensible heat fluxes, net radiation at the soil surface and vapor pressure deficit.

The boundary conditions of watershed scale climate simulations are based on the predictors of global climate models (GCMs with ~200x200 km tiles), and can be obtained for the watershed scale by either (Mpelasoka and Chiew, 2009) (i) empirical downscaling of historical data informed by GCM simulations, (ii) by statistical downscaling of GCM predictors, or (iii) by dynamic downscaling of GCM predictors using regional climate models (RCMs). Statistical and dynamic downscaling are often preferred for two reasons: firstly, they can account for changes in the weather characteristics and synoptic patterns that may apply for future climate, and secondly, GCMs are not optimised for the purpose of simulating rainfall but rather for simulating large-scale atmospheric simulation.

The approach defined for our study is based on simulations of the Canadian Regional Climate Model (CRCM; Caya and Laprise, 1999; Music and Caya, 2007), which is in a dynamical downscaling of GCMs to the regional scale. The daily translation (DT) method will subsequently be used to perform an empirical downscaling where rainfall forecasts from CRCM are calculated for the watershed scale using a relationship between the historical meteorological variables on the CRCM-scale and historical meteorological data for the study area. The historical data include observations by the St. Paulin weather station of the MDDEP (Ministère du Développement Durable, de l'Environnement et des Parcs - Ministry of Sustainable Development, Environment and Parks of the province of Quebec), located at 4 km SSW of the study site and operational from 1950-1991. For the period 1991-2010 Ouranos plans on using historical data from other nearby stations, such as Charrette (7.8 km WSW of the study site), Shawinigan, St.-Alexis-des-Monts and Trois Rivières (1950-present). Meteorological variables measured by these stations will be interpolated for the study site using the geostatistical (ordinary) Kriging method. Weather data for the 2011 growing season were obtained directly at the study site by our own weather station, and can also be used in the downscaling process.

Cluster analysis of selected meteorological variables will allow for the selection of the simulation periods, which will for each simuation include a growing season (April-November), with a maximum variation in the values of these selected variables. The maximum variations of these variables will form the selection criteria for two to six climate simulations of growing seasons between 2041-2070 with a time step duration of one day, and could include rainfall and degree days, which is the summed temperature in excess of 5 degrees C for the growing season.

Once the selection criteria are defined and applied, downscaling can begin. Eventually, this downscaling may be applied to the whole set of available climate simulations, including GCMs, RCMs and simulations calculated for the NARCCAP (North American Regional Climate Change Assessment Program). Multiple simulations allow for a better identification of their respective

uncertainties and thus yield more robust conclusions (Murphy et al., 2009). This method seems particularly useful in view of the high spatial resolution of the soil water distribution model.

1.3 List of contributors and partners

The following persons participate on behalf of INRS-ETE (Quebec):

Alain N. Rousseau Professor (local management, hydrological modelling, field study)

Silvio J. Gumiere Postdoctoral fellow, currently assistant professor at Université Laval (May-July 2011, hydrological modelling, field study)

Dennis W. Hallema Postdoctoral fellow (since November 2011, hydrological modelling and field study)

Grégor Levrel Ph.D. student (FDR measurements)

Gwenael Carrer Ph.D. student (weather data)

Maxime Fossey Ph.D. student (grain size analysis)

Partners at the Centre d'étude de la Forêt (CEF, UdeM):

Alain Paquette Professor (field logistics, biology)

Susy Domenicano Ph.D. student (biology, modelling)

Léa Bouttier Data readout

Partners at Université Laval:

Alain Olivier Professor (project administrator)

Silvio J. Gumiere Assistant professor (hydrological modelling and field study)

Sylvain Jutras Professor (grain size analysis)

Partners at the Institut de Recherche en Biologie Végétale:

Alain Cogliastro Associate professor (ecology and biology)

1.4 Outline

The document continues with a detailed presentation of our activities in the pursuit of our objectives. First, we provide an overview of materials and methods, followed by preliminary field results and the modelling approach that we plan to follow in 2012. In the latter we will explain into detail the modelling approach that we adopted for simulating soil water dynamics.

Chapter 2

Field study

2.1 Description of the St. Paulin research site

Measurements were performed in the Rivière du Loup-Lac Saint-Pierre watershed near Le Baluchon Inn, located at 25 km NNW of Lac Saint-Pierre within the municipality of St. Paulin in Mauricie, QC Canada (Figure 2.1). The approximate coordinates are 46°27'10" N 72°59'30" W and elevation is around 142 m. The site is located on Juneau Island, which is formed by the land enclosed between two branches of the Rivière du Loup that splits 1 km downstream of Hunterstown and merges again 600 m upstream of the "Chute aux Chaudières" waterfall. The east bank (altitude 200 m) is an alluvial terrace with sandy material and gravel, whereas the west bank (altitude 160 m) and Juneau Island are characterised by loamy and clayey marine sediments, which were deposited when the region was covered by a water body known as the Champlain Sea (Figure 2.2). The river bed is cut into the marine sediments to an altitude of around 125 m at Juneau Island, which represents a depth of around 17-18 m with respect to our field site.

This site was selected for two reasons: (i) agriculture is practiced according to the alley cropping system, which requires the planting of trees at wide spacings creating alleyways within which crops are grown (Garrett et al., 2011); and (ii) the alley cropping system was already an active research site for research on the contribution of multifunctional agroforestry systems to the climate change adaptation capacity of agro-ecosystems (professor Alain Olivier, Laval University).

2.2 Materials and methods

2.2.1 Weather station

A weather station was mounted in the study area to measure air pressure, photosynthetically active radiation (PAR, 400 to 700 nm), wind speed, wind direction, air temperature, relative humidity, and rainfall. The weather station was positioned at approximately 120 m from the FDR setup in a suitable clearing, in order to prevent disturbance of measurements caused by the presence of trees and other high features.

The following components were purchased and installed at the field site on 2011-05-17 (an overview):

- Monitoring: One independent monitoring system Onset Hobo U30 with space for a battery. This system operates under temperatures from -20 to 40 degrees C, has 10 Smart Sensor ports and 15 channels. Data and can be downloaded over a USB connection (mini-USB) using the Hoboware Pro software (Windows and MacOS). A LED indicates whether the system is logging

Figure 2.1: Satellite image of the St. Paulin study area in the administrative region of Mauricie, QC (Cnes/Spot/Google).

or not. Includes one 4 V 10.0 Ah battery (Power Sonic type PS-4100) and 100 m of cable. Cost: $457.00 plus $98.25 for the Hoboware Pro software.

- Power unit charged using one solar panel providing 1.2 W (Onset Solar). Cost: $85.00
- Relative humidity measurements: Onset S-THB-M002 Smart Sensor hygrometer for measuring relative humidity (1-100%) and temperature (-40 to 75 degrees C). Includes cable of 2 m length. Cost: $196.00
- Wind speed and direction: Onset S-WCA-M003 combined anemometer and wind vane for wind speed between 0-44 $m.s^{-1}$ and wind direction between 0-358 degrees (threshold wind speed to measure the latter is 0.5 $m.s^{-1}$) mounted on an Onset M-CAB half cross arm connected to the tripod. Cost: $617.00 (anemometer-wind vane) plus $51.50 (half cross arm)
- Rain gauge: Onset S-RGB-M002 tipping bucket rain gauge (0.2 mm container), with 2 m cable. Cost: $469.00
- Air pressure sensor: Onset S-BPB-CM50 Smart Sensor for measuring barometric pressure from 660-1070 mbar with an accuracy of 0.1 mbar and 50 cm cable. Cost: $258.50
- Sensor of photosynthetically active radiation (PAR): Onset S-LIA-M003 detecting 400 to 700 nm (visible radiation), with 3 m cable. Cost: $228.00 (PAR) plus $33.00 (Onset M-LBB light sensor bracket)
- Solar radiation shield: Onset RS3, protects sensors (relative humidity, air temperature) from sunlight. Cost: $67.00

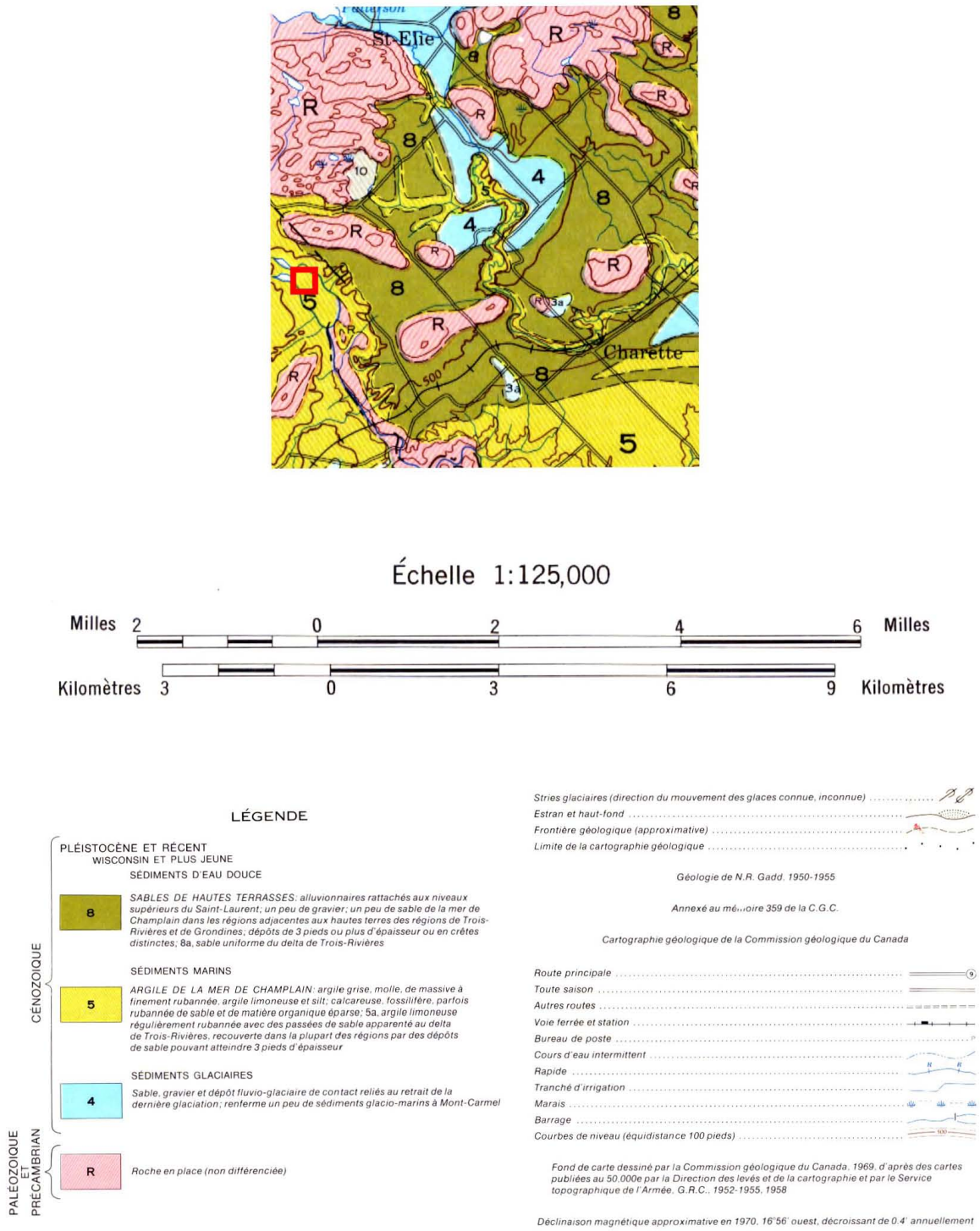

Figure 2.2: The geology of the study site is characterised by loamy marine sediments. The study site itself is marked by the small red square on the right hand side (excerpt of geological map 1197A, Geological Survey of Canada, 1971).

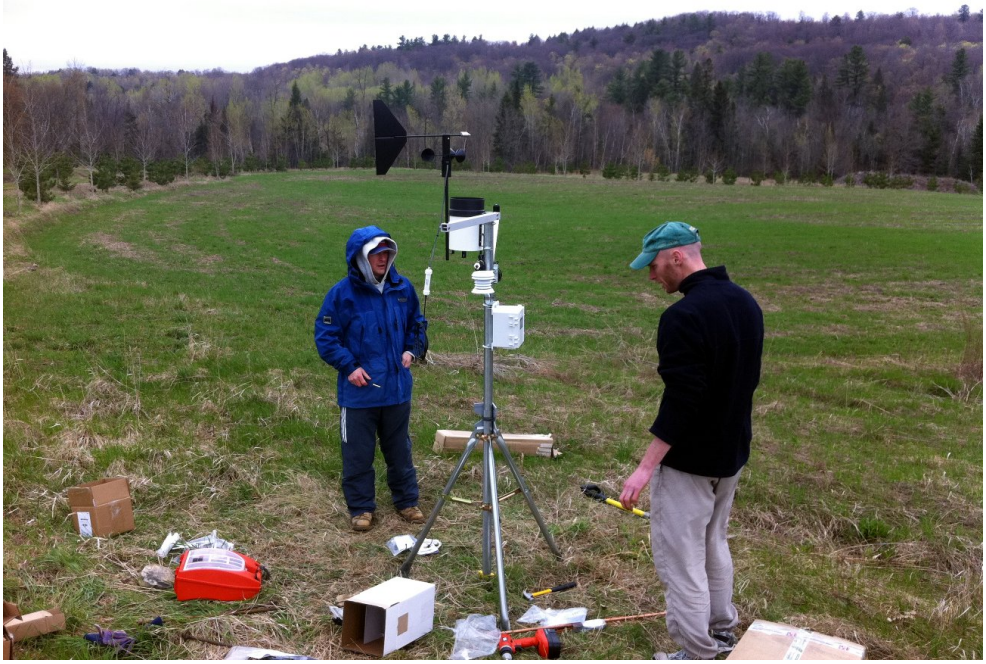

Figure 2.3: Setting up the weather station. On this photo we see the following components attached to the tripod (from top to bottom): wind vane, anemometer, pluviometer, hygrometer, monitoring system. After this photo was taken, the weather station was attached to the ground using guy wires.

- Tripod on which the weather station is mounted: Onset M-TPB-KIT, which includes a 2 m metal tripod (M-TPB), a mast level (M-MLA), guy wire kit (M-GWA), 1/2" stake kit (M-SKA) for guy wires, 1/4" stake kit (M-SKB) for tripod and a grounding kit (M-GKA). Cost: $234.00

The total of the above purchase amounts to $2794.25. Additional costs include various tools and materials to install the weather station and attach it to the ground.

The measurement period lasted from 2011-06-09 to 2011-11-10 (5 months), during which one data entry was recorded every 15 minutes, based on the average measured value over the last minute of each such 15 minute cycle. We returned to the field site on 2011-11-10 to unmount the weather station and bring it back to the INRS-ETE in Quebec for hibernation. All equipment except the anometer/wind vane was left attached to the weather station, so that the second season it can be up and running within half an hour.

2.2.2 Grain size analysis

We performed a grain size analysis of a soil sample taken from the study site. The resulting grain size distribution provides an indication of the grain size distribution elsewhere in the alley cropping system. We followed the standard method of particle-size analysis of soils (ASTM D-322) as approved by the American National Standard Institute and described by the Canadian Soil Survey Committee (American National Standard Institute, 1972; Comité Canadien de Pédologie, 1978). This method prescribes the dry sieving of the sand fraction after sedimentation in water. The method for quantifying organic matter is based on the loss on ignition (LOI) at 375 °C, as described by the Centre

d'Expertise en Analyse Environnementale du Quebec.

2.2.3 Frequency domain reflectometry (FDR) for measuring soil moisture patterns

We used frequency domain reflectometry (FDR) to measure moisture patterns within the first 100 cm of the soil. A total of 45 FDR sensors were divided into 11 sets on a plane perpendicular to the tree rows (see Figure 2.4). Each set is composed of 2 to 5 FDR sensors measuring the volumetric soil water content at five different depths up to 100 cm below the soil surface and hence each set represents one vertical soil moisture profile. The FDR sensors of a given set were aligned with the tree rows, so that all sets combined provide a two-dimensional soil moisture profile in a plane perpendicular to the tree rows. This will give us a dynamic image of the soil moisture distribution in this plane, which will be useful for evaluating our upcoming modelling study of this hydrodynamic system.

The 45 FDR sensors were installed as follows. First, we drilled 45 holes in the ground using a hand auger with a 5 cm diameter, where all boreholes in one set are in the same vertical plane parallel to the tree rows spaced at 20 cm. The holes were cleaned during and after drilling using a soft brush, resulting in boreholes with a stable shaft free of drilled material (illustrated in Figure 2.5). Subsequently, the sensors were inserted vertically into the soil at the bottom of the boreholes. Each set has 3-5 sensors, denoted A to E, at different depths below the surface: 7 cm, 25 cm, 45 cm, 75 cm, 100 cm. These depths correspond with the middle of the probe (exposed part of the sensor), which consists of two pins. The sensors were connected to one of the three monitoring systems using extension cables (Figure 2.6). Lastly, each borehole was filled with the same material that was removed earlier. The measurement period was from 2011-06-09 through 2011-11-10, after which the equipment was left at the site.

The following components were purchased and used in the setup:

- Moisture sensors: 46*FDR sensor type Onset S-SMD-M005, 10HS, 70 MHz, volume of influence 1 liter. The high frequency circuit reduces sensitivity to salinity. Each sensor has a unique frequency around 70 MHz, and the distance between two sensors within one set was chosen such as to avoid signal interference (>20 cm). This, together with the probe length of 10 cm being a few centimeters longer compared to other more sensitive sensors, helps averaging out any variability in soil moisture patterns within 1 dm^3 of soil. Operates between 0-50 degrees C. Cost: 46*$159.25=$7325.50

- Monitoring: Three independent monitoring systems Onset Hobo U30 with space for a battery. This system operates under temperatures from -20 to 40 degrees C, has 10 Smart Sensor ports and 15 channels. In combination with a Smart Sensor consolidator box it was possible to record the data of 15 FDRs per monitoring system. The frequency of measurements was one record per 15 minutes, based on the average measured value over the last minute of each 15 minute cycle. Data and can be downloaded over a USB connection (mini USB) using the Hoboware Pro software (Windows and MacOS). A LED indicates whether the system is logging or not. Includes three 4V 10.0 Ah batteries (Power Sonic type PS-4100) and 3*100 m of cable. Cost: 3*$457.00=$1371.00 (the price of the required Hoboware Pro software is already included in the total cost for the weather station; see above)

- Each of the three power units is charged using a solar panel providing 1.2 W (Onset Solar). Cost: 3*$85.00=$255.00

- Smart Sensor consolidator box Onset S-ADAPT-6, in order to be able to connect up to 6 smart sensors in a water-resistant enclosure to one sensor extension cable back to a Hobo U30, thus extending the number of smart sensors that can be connected to one monitoring system from 10 to 15. Cost: $109.00

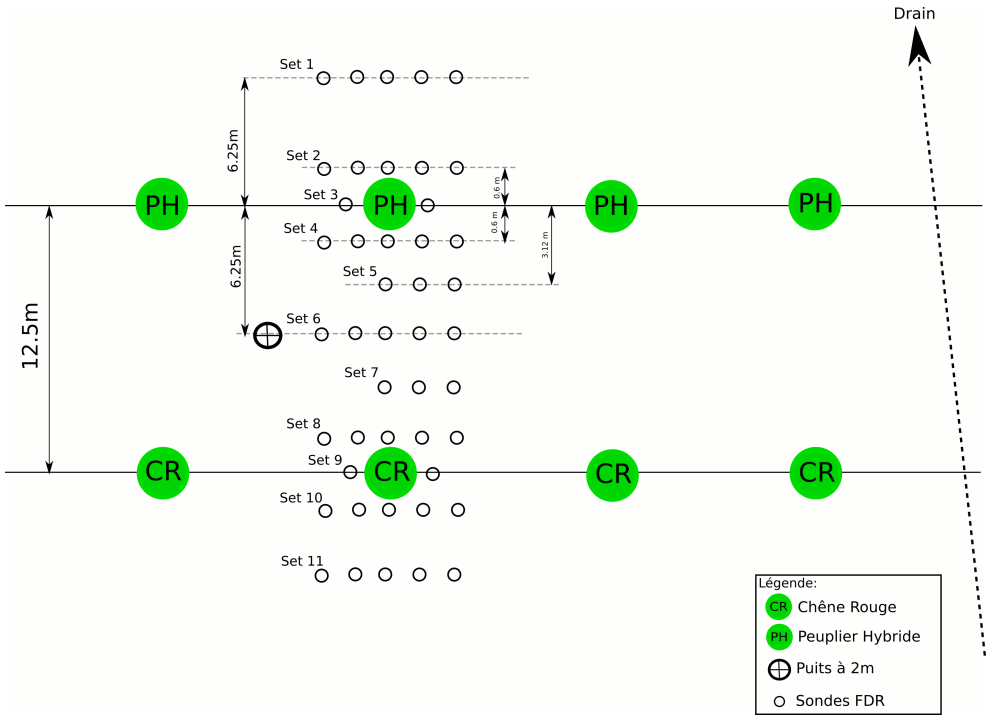

(a) Plan view

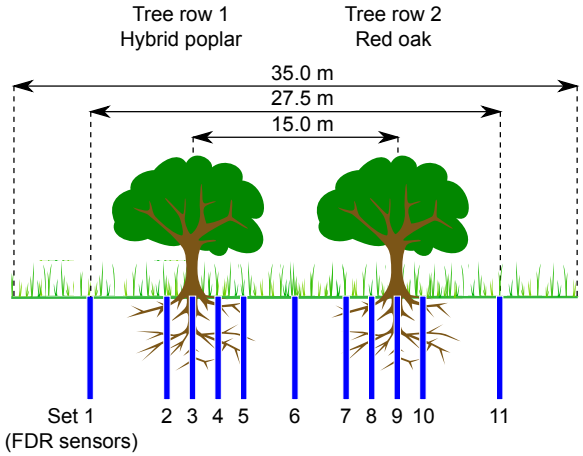

(b) Transect

Figure 2.4: Plan view and transect of the FDR setup (not to scale). The FDR sensors were divided into sets on a plane perpendicular to the tree rows. Each set is composed of 2 to 5 FDR sensors measuring soil water content at different depths: 7, 25, 45, 75 and 100 cm below the soil surface. Hence each set represents one vertical soil moisture profile.

(a) Drilling a hole with a 5 cm hand auger

(b) Cleaning the freshly drilled hole with a brush

(c) The resulting borehole is free of drilled material

Figure 2.5: Drilling holes for the FDR sensors.

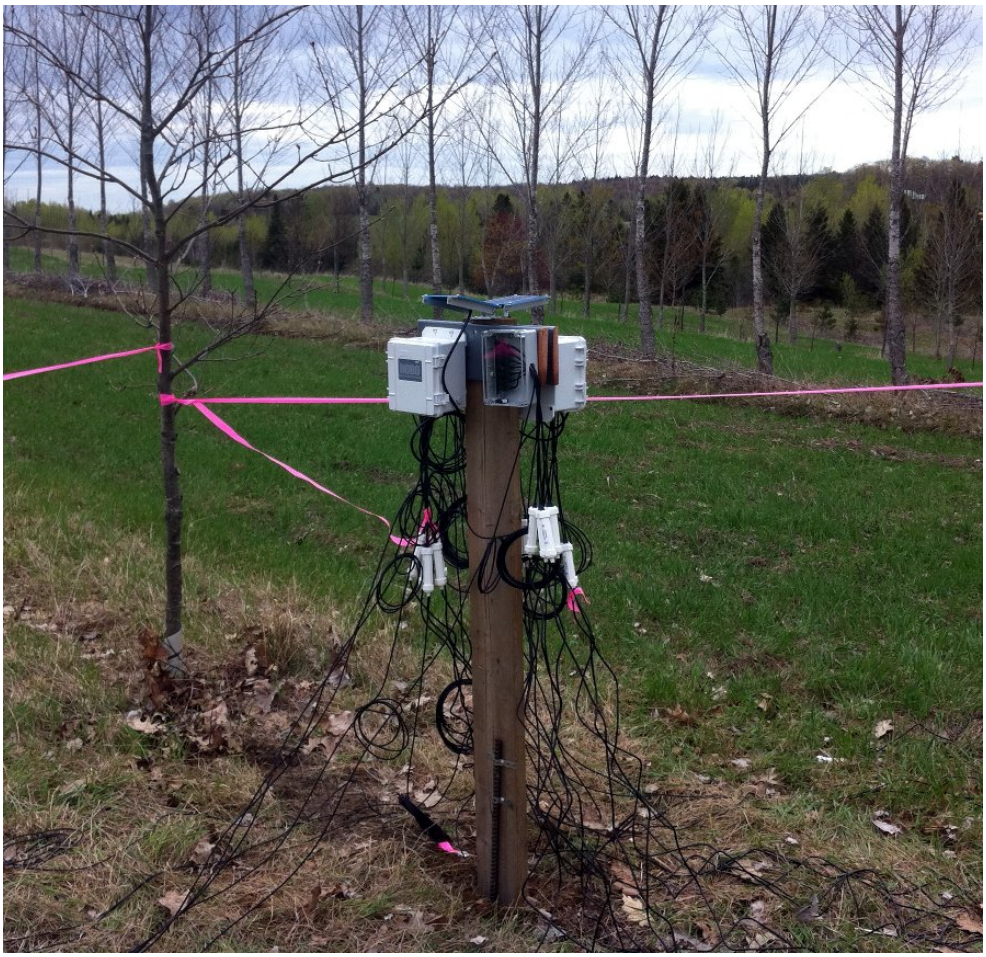

Figure 2.6: Two Onset Hobo U30 monitoring systems mounted on a wooden support firmly attached to the soil.

- Extension cables: 15*Onset S-EXT-M005, 5 m Smart Sensor male-to-male extender cable, plus a female-to-female adaptor. Cost: 15*$28.25=$423.75
- Extension cables: 6*Onset S-EXT-M010, 10 m Smart Sensor male-to-male extender cable, plus a female-to-female adaptor. Cost: 6*$34.00=$204.00
- Additional sensor: water pressure sensor Solinst Levellogger LT F30/M10, model 3001.

Total of the above purchase amounts to $9688.25. Additional costs include tools and materials to install the equipment.

2.3 Preliminary results

2.3.1 Weather data

We now present the data obtained with the weather station at the field site in St. Paulin, QC. Data could be retrieved from all sensors, and all data are within their respective plausible ranges during the *measurement period running from 2011-06-09 through 2011-11-10 (5 months).*

2.3.1.1 Rainfall

Rainfall was 618 mm in total, distributed over 30 rainfall episodes with a rainfall intensity of more than 2 mm per 15 minutes. These rainfall episodes are nearly uniformly distributed over the duration of the summer and autumn of 2011, with August being the wettest month with 188.2 mm and July and October being the driest months, with 95.4 and 96.8 mm, respectively (Table 2.1 and Figure 2.1).

2.3.1.2 Photosynthetically active radiation (PAR) and temperature

PAR values were highest in the week of the summer solstice in the northern hemisphere (which took place on 2011-06-21) with values around 2400 $\mu mol.m^{-2}.s^{-1}$ during the day, and decline toward the winter. Our data runs until 2011-11-10, where values peak around 1000 $\mu mol.m^{-2}.s^{-1}$ during the day (Figure 2.8). Maximum PAR was recorded at 2553.7 $\mu mol.m^{-2}.s^{-1}$ on 2011-07-01 at 12:43, which is a little out of the measurement range 0-2500 $\mu mol.m^{-2}.s^{-1}$ specified by the sensor's manufacturer. Note that the PAR sensor data cannot be converted to solar radiation ($W.m^{-2}$) since it only samples radiation with a 400-700 nm wavelength.

July 2011 was the hottest month with an average temperature of 20.4 $°C$, while October 2011 was the coldest month with 7.6 $°C$ on average (Table 2.2 and Figure 2.9). The highest temperature was measured on 2011-07-22 at 14:52 (32.3 $°C$), lowest temperature on 2011-11-06 at 07:37 (-7.5 $°C$).

2.3.1.3 Relative humidity and atmospheric pressure

Relative humidity is often close to 100% during the night (Figure 2.10). The relationship between relative humidity, atmospheric pressure and air temperature is illustrated for 2011-09-01 in Figure 2.11: the decrease in barometric pressure between the first and second midnight would for a given temperature lower the dew point and increase relative humidity. However, temperature increased from 11.4 $°C$ to 13.8 $°C$ over the same period, thus offsetting the effect of a decrease in barometric pressure and effectively reducing relative humidity to subsaturation levels (98.9%).

Longer term tendencies for air pressure demonstrate a relationship with air temperature (cf. Figures 2.12 and 2.9): an increasing air pressure between 2011-10-05 and 2011-10-07 from 1000 mbar to 1012 mbar was followed by three warm days with temperatures rising to 25.2 $°C$, 26.1 $°C$ and 20.6 $°C$ on 2011-10-08, 2011-10-09 and 2011-10-10, respectively. Wind direction during this week was predominantly southeast with stronger than usual gusts.

Month	Rainfall (mm)
July 2011	95.4
August 2011	188.2
September 2011	110.4
October 2011	96.8
Total rainfall (mm)	490.8

Table 2.1: Monthly rainfall at St. Paulin.

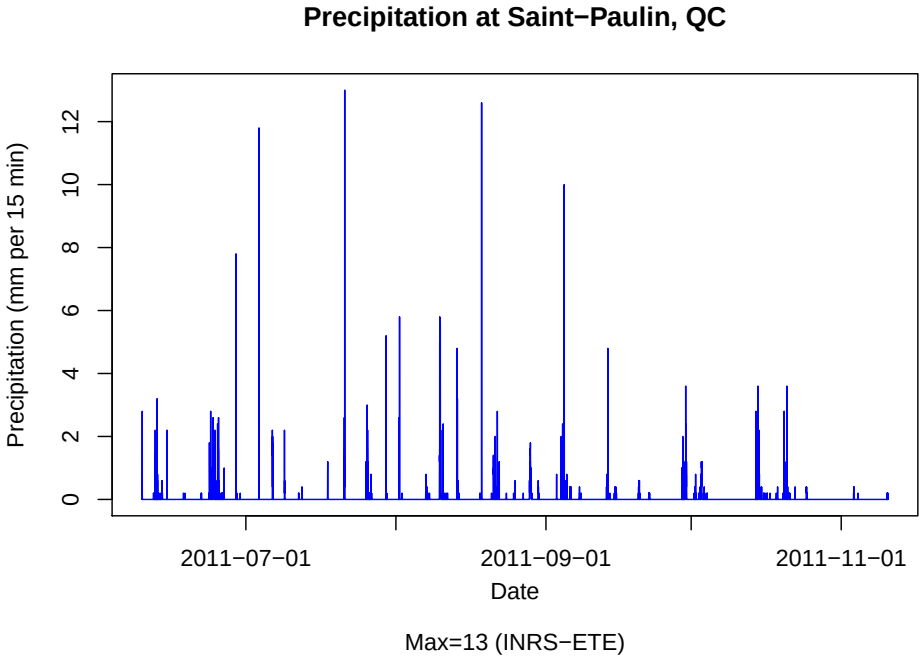

Figure 2.7: Rainfall measured at St. Paulin.

Month	Mean temperature ($°C$)
July 2011	20.4
August 2011	18.1
September 2011	14.6
October 2011	7.6
Monthly average ($°C$)	15.2

Table 2.2: Mean temperature at St. Paulin.

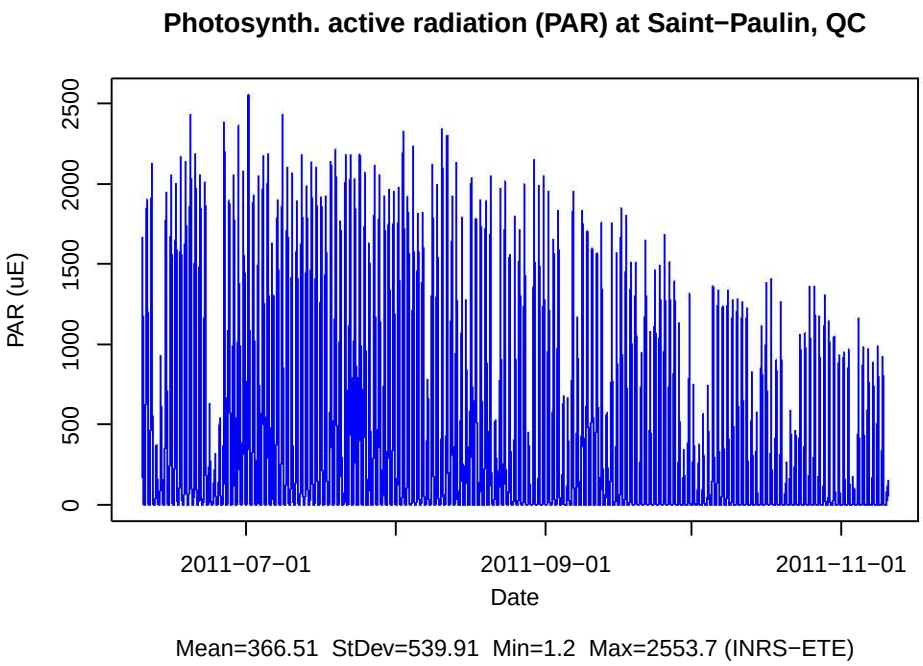

Figure 2.8: Observed PAR (photosynthetically active radiation).

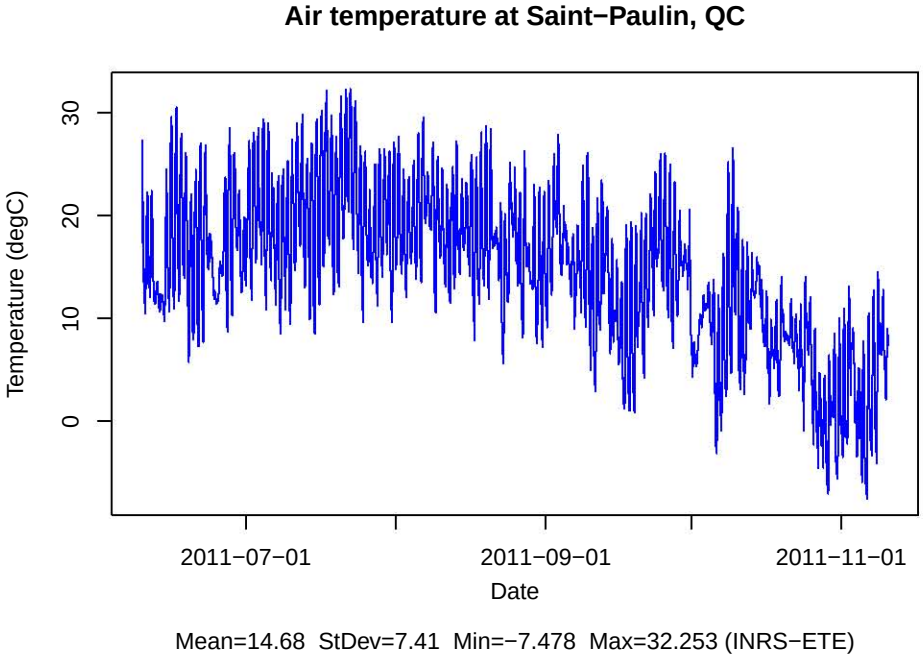

Figure 2.9: Air temperature.

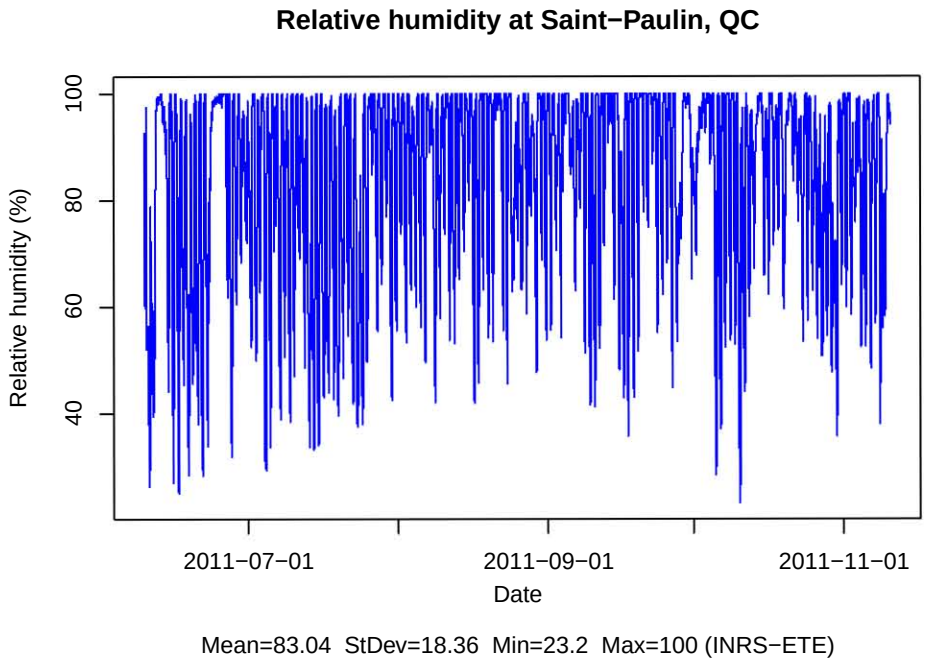

Figure 2.10: Relative humidity.

2.3.1.4 Wind speed and direction

Figure 2.13a shows a wind rose that is based on the average wind during 1 minute, sampled four times per hour. Most of the time wind came from SSE to ESE, which is the direction of the Saint-Lawrence River. Recorded wind speed are quite slow compared to wind speeds observed in regions closer to the sea, and can be classified as gentle breeze at most (wind speed up to 6 $m.s^{-1}$, which corresponds to Beaufort scale 3). Cold winds coming from NNW-NW were mostly light breezes up to 4 $m.s^{-1}$ (Beaufort scale 2-3). Wind gusts coming from SSE-ESE were strongest, with speeds up to 15-16 $m.s^{-1}$ (Beaufort scale 7; see also Figure 2.13b).

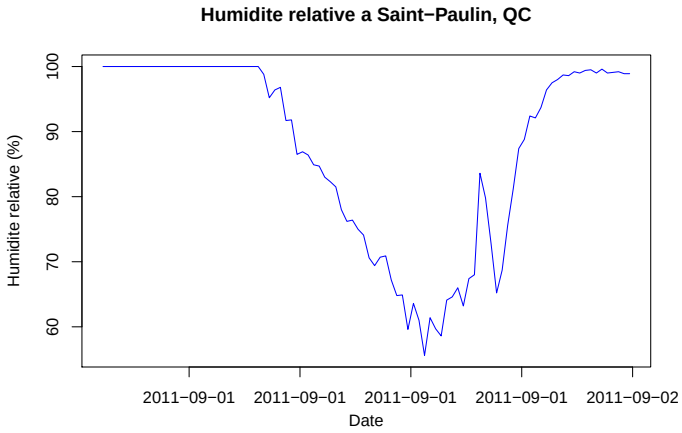

(a) Relative humidity on 2011-09-01.

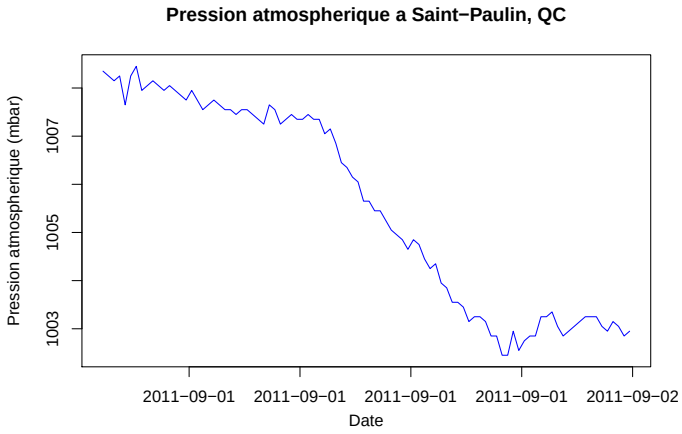

(b) Air pressure on 2011-09-01.

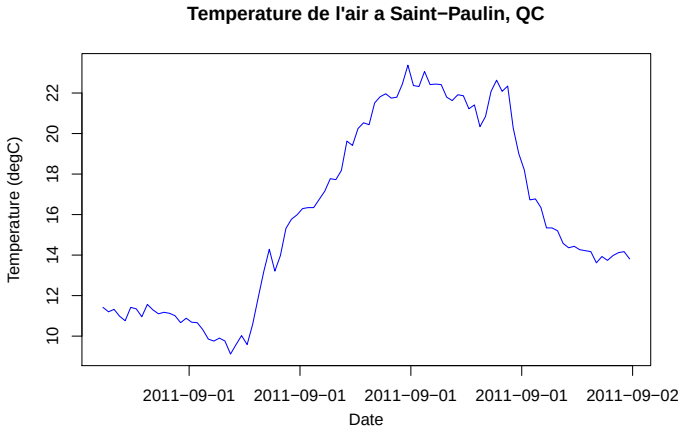

(c) Air temperature on 2011-09-01.

Figure 2.11: Comparison of relative humidity, air temperature and air pressure at St. Paulin for a given period of 24 hours.

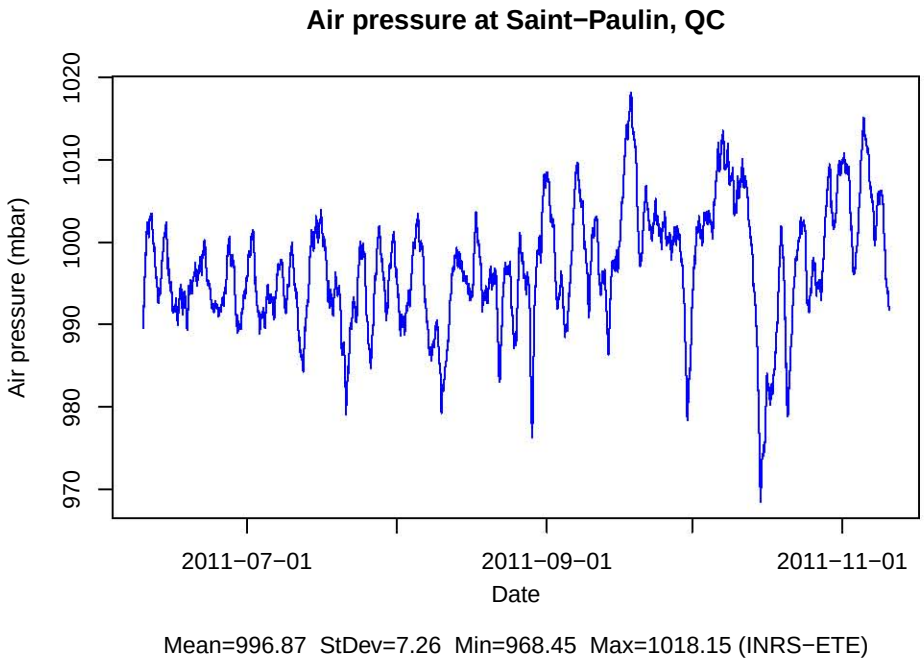

Figure 2.12: Air pressure.

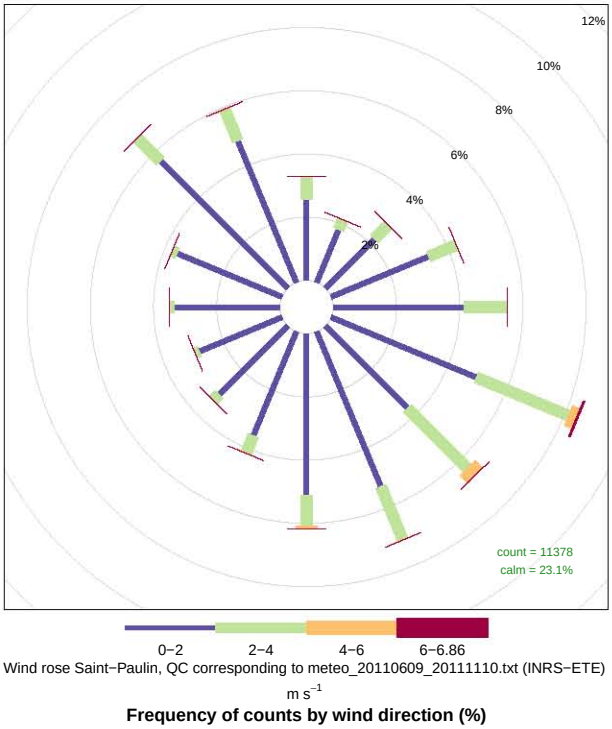

(a) Wind rose calculated for one-minute time intervals.

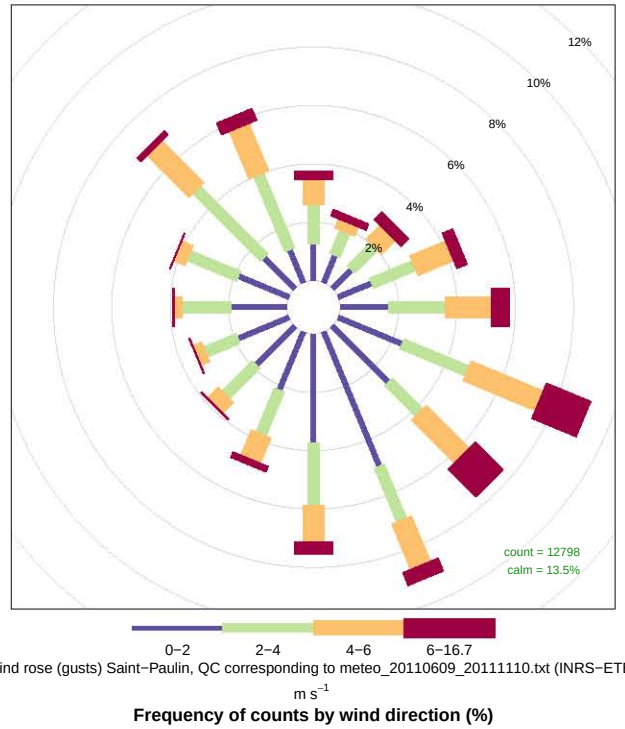

(b) Wind gusts.

Figure 2.13: Wind roses for St. Paulin, based on measurements between 2011-06-09 and 2011-11-10.

2.3.2 Grain size analysis

The results of the grain size analysis or shown in Tables 2.3, 2.4 and 2.5. The soil can be classified as a sandy soil with traces of silt, which corresponds with the sandy soils found by Bambrick et al. (2010). An additional analysis was carried out to determine the amount of organic matter in the soil (results in Table 2.6).

Identifiant	Classes granulo	
	Sable total 1mm>x>0,05mm	Limon 0,05mm>x>0,002mm
0 – 15	87	8
15 – 25	89	8
25 – 35	88	6
35 – 45	95	2
45 – 60	95	2
60 – 75	96	2
75 - 100	41	37
120 - 140	37	28

Table 2.3: Grain size analysis of the soil sample taken at the study site near St. Paulin, QC.

Horizon	Type de sol
0 - 15	Sable loameux
15 - 25	Sable
25 - 35	Sable
35 – 45	Sable
45 – 60	Sable
60 – 75	Sable
75 - 100	Loam
120 - 140	Loam argileux

Table 2.4: Texture classes corresponding with the different soil layers.

Identifiant	Classes granulométriques			
	Sable très grossier 2 mm > x > 1mm	Sable grossier 1mm>x>0,5mm	Sable moyen 0,5mm>x>0,25mm	Sable fin 0.25mm>x>0.1mm
0 – 15	1	16	43	36
15 – 25	2	17	42	35
25 – 35	2	21	40	34
35 – 45	4	36	38	22
45 – 60	1	18	56	24
60 – 75	1	8	61	29
75 - 100	0	12	28	19
120 - 140	3	16	21	17

Table 2.5: Grain size distribution of the fraction >0.1 *mm* after dry sieving.

Horizon	Pourcentage de Matière Organique (%)
0 - 15	2,9
15 - 25	3,6
25 - 35	2,9
35 – 45	1,4
45 – 60	0,9
60 – 75	0,6
75 - 100	0,3
120 - 140	0,9

Table 2.6: Organic matter of the soil sample (per cent).

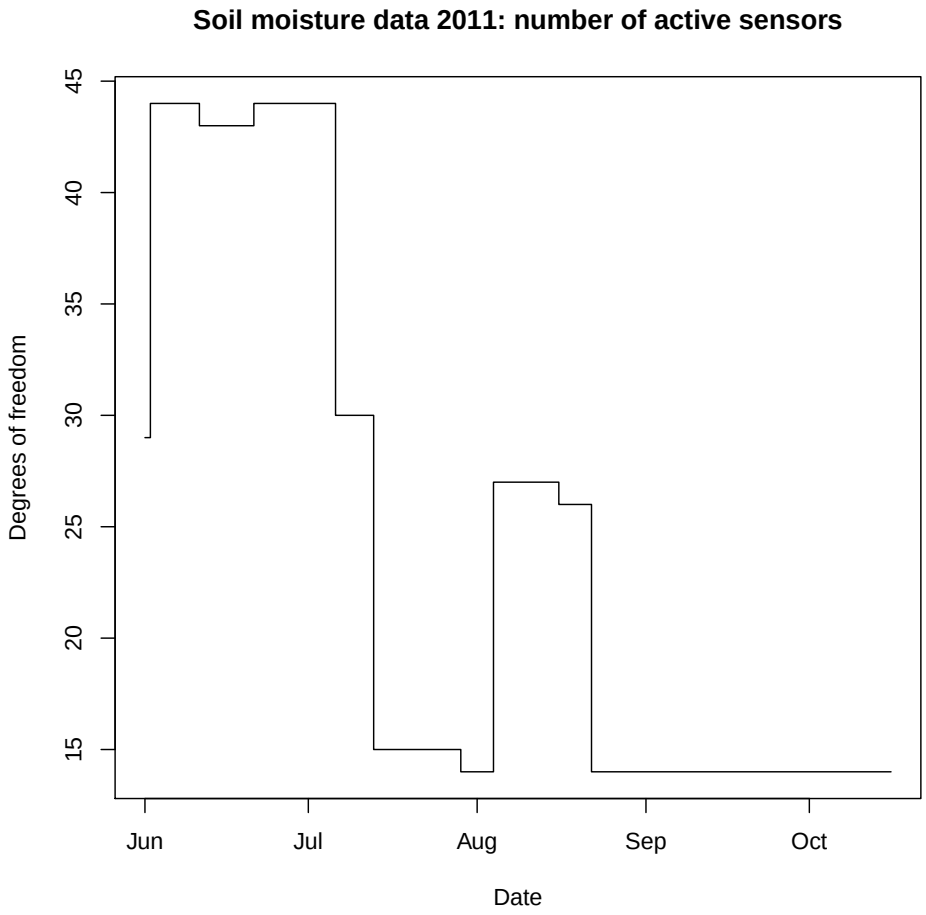

Figure 2.14: Number of active FDR sensors during the measurement period.

2.3.3 Soil moisture patterns (FDR data)

Data was retrieved from the FDR monitoring systems on 2011-11-10; the number of active sensors during the measurement period is shown in Figure 2.14.

A first comparison between volumetric water content for set 1 and 2 below a depth of 70 cm (Figures 2.15 on page 28 and 2.16 on page 29) show that the soil at this depth is generally dryer close to the tree (set 2; position indicated in Figure 2.4 on page 14). Similar comparisons hold true for other sets as well, which may indicate that most water is extracted below this depth closer to the tree. Temporal variations in volumetric water content provide process information as well: the jagged water content for set 2 at a depth of 7 cm, between time step 1350-1600, could be the result of stem flow that reaches the ground, and the oscillations may be directly related to rainfall intensity.

After classification of the grain size we found that the layer below a depth of 75-100 cm has a loam to clay loam texture (below 120 cm; compare Table 2.4 on page 24). Local sediments being of lacustrine origin (geological map by the Commission Géologique du Canada, 1971), we may assume that deposition of individual layers including the clay loam layer at a depth of 120 cm was more or less horizontal. We expect therefore that variations in water content with depth are not only due to water uptake by vegetation within the first meter below the surface, but also due to the formation

of a perched water layer above the less conductive clay loam layer at a depth of 120 cm. We expect that further analysis will provide more information on this issue.

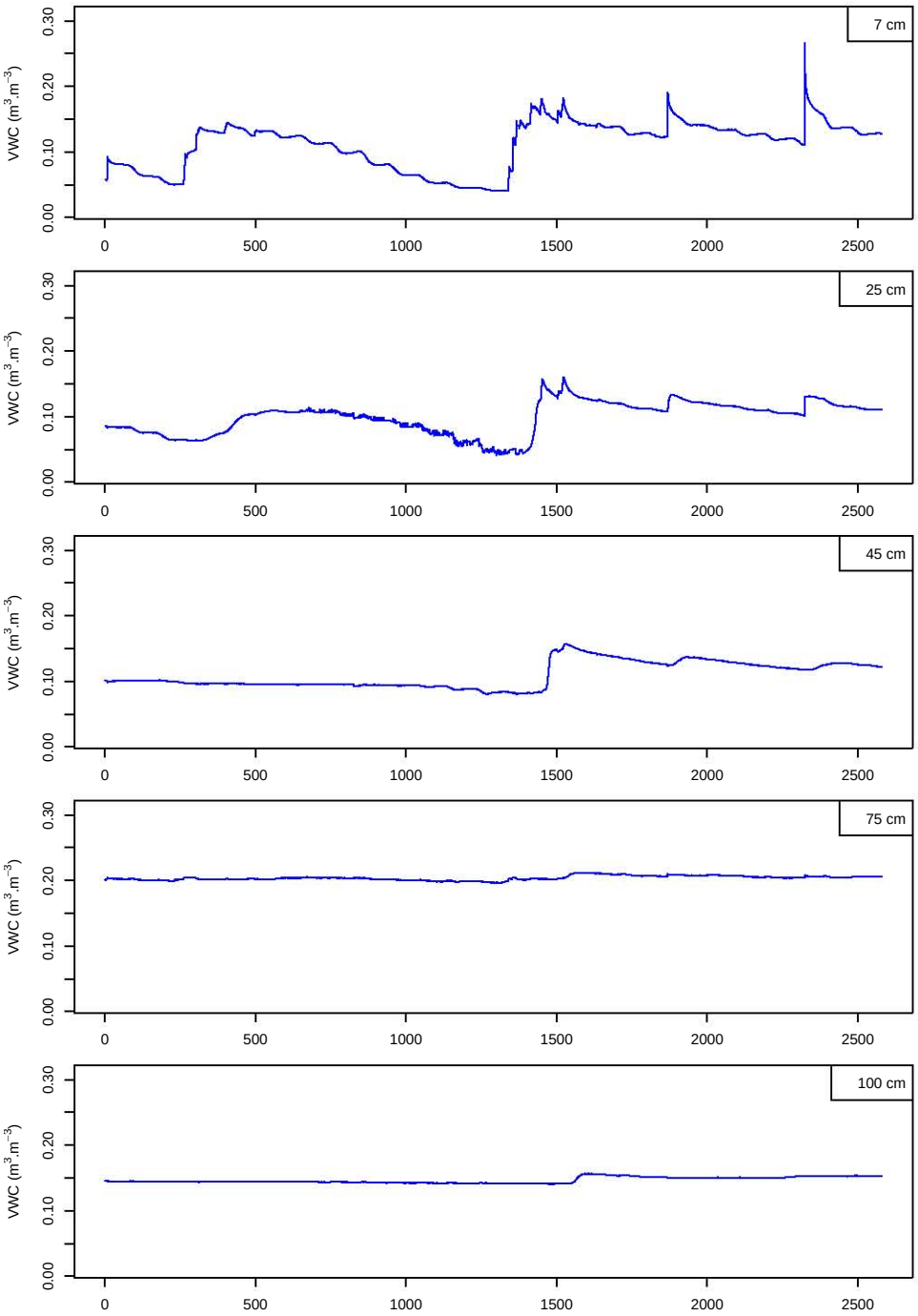

Figure 2.15: Volumetric soil water content for set 1 observed by FDR sensors between 2011-06-09 and 2011-07-06 (compare Figure 2.4 on page 14). Temporal variations were most apparent above 75 cm of depth.

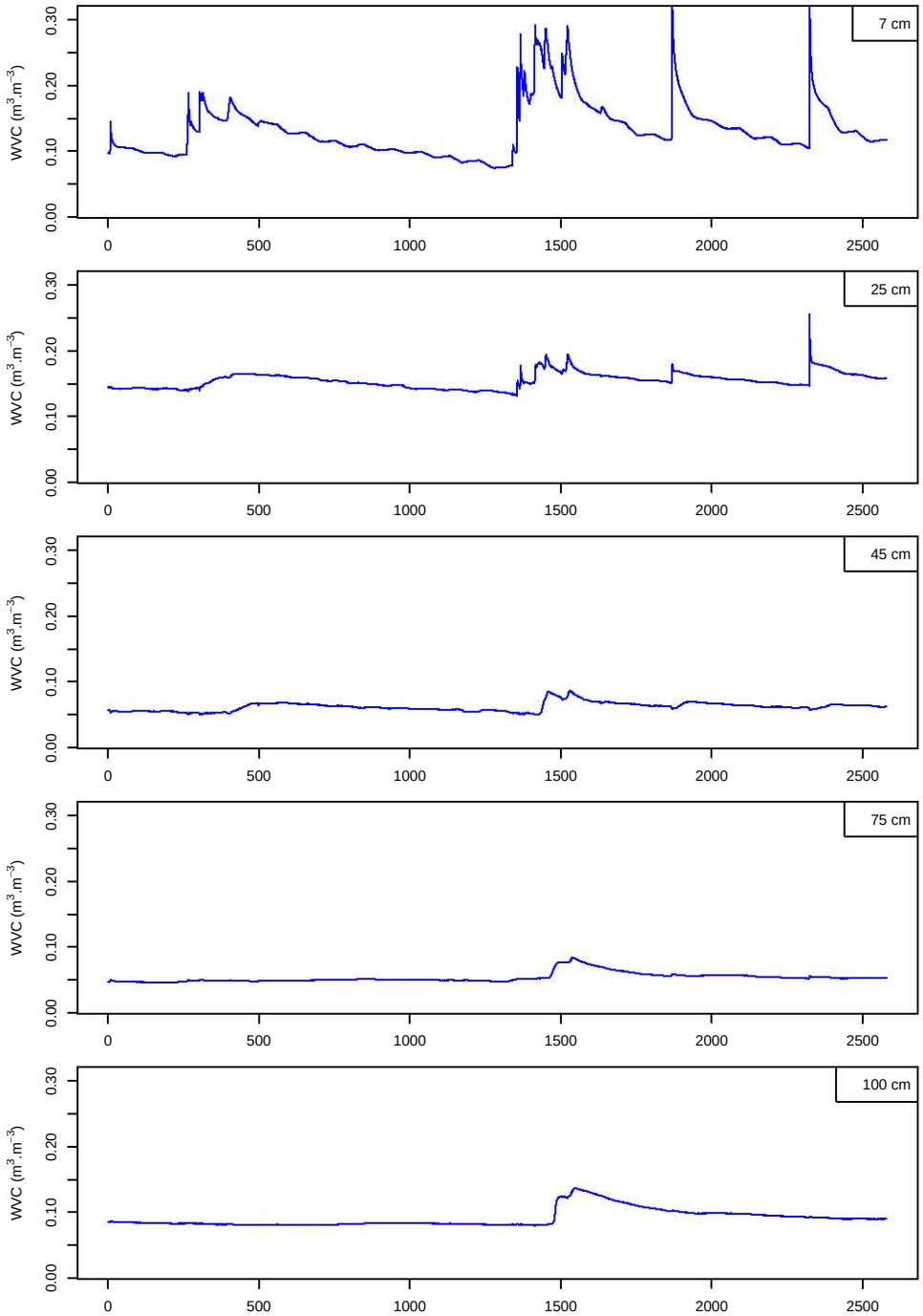

Figure 2.16: Volumetric soil water content for set 2 observed by the FDR setup between 2011-06-09 and 2011-07-06. Temporal variations are observed throughout the soil profile.

Chapter 3

Modelling soil water dynamics

In response to our objective to quantify the effect of alley cropping systems on soil water dynamics and water erosion, we earlier proposed a three-fold method based on modelling: (i) soil water dynamics, (ii) soil erosion by water, and (iii) different climate change scenarios. Currently, we have completed the 2011 field campaign, which included weather observation and soil moisture monitoring for an alley cropping site in Mauricie, in the Canadian province of Quebec.

Now that the field campaign is complete we can continue with the final phase of the first part where our objective is:

> To quantify and evaluate the effect of alley cropping systems on soil water dynamics at the plot scale (15 m transect).

Our hypothesis is that the root systems of the trees interact with soil water dynamics, i.e. root systems tend to grow in the direction of soil layers with a water content corresponding to a pF between 2-2.4, and conversely, soil water flows in the direction of decreasing hydraulic head, which, close to the root system, is in the direction of the roots when the trees absorb water by means of suction. In order to test this hypothesis and evaluate the interaction between root system and soil water dynamics, we adopt an approach divided into three steps:

1. Analyse and prepare the weather data, soil texture data and soil moisture data obtained during the 2011 field campaign at an alley cropping system near St. Paulin (Mauricie, QC Canada). Select a rainfall episode that is representative of the measurement period in terms of rainfall amount and intensity.

2. Simulate soil water dynamics of the alley cropping system (scenario A) for the selected rainfall episodes. We will use three process-based models:

   (a) Variably saturated flow in the soil: Richards equation (Richards, 1931)

   (b) Transpiration throught root uptake by vegetation: Feddes linear water stress response function (Feddes et al., 1978, 2001) and the nonlinear water and osmotic stress response function in combination with time-variable rooting depth (Hoffman and Van Genuchten, 1983)

   (c) Evaporation from the soil surface: Penman-Monteith equation (Penman, 1948; Monteith, 1981)

3. Model soil water dynamics for a virtual situation that is comparable to the above system, but without alley cropping (scenario B). This subsequently allows for a comparison of soil water dynamics for scenarios A and B.

The modelling environment that we will use to quantify and evaluate the effect of alley cropping systems on soil water dynamics at the plot scale is HYDRUS 2D/3D.

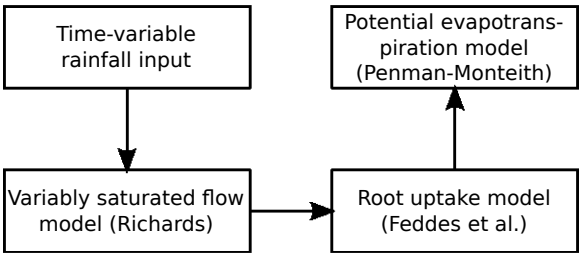

Figure 3.1: Model structure

3.1 Process modelling

In case of rainfall, the hydrologic response of an alley cropping system is characterised by the following hydrological processes. First rainfall infiltrates into the soil surface and from there moves vertically and laterally through the soil (infiltration, throughflow). This phenomenon is simulated using the Richards equation for variably saturated flow. Subsequently, water can be stored in pore spaces, leave the soil system by percolation to the groundwater table, be taken up by roots (potential transpiration), or evaporate directly from the soil surface.

We have selected three models that are able to simulate these processes observed in the soil (up to 1.5 m depth), which are (i) the nonlinear Richards equation for variably saturated flow in the soil, (ii) Feddes linear water stress response function for simulating water uptake by roots, and (iii) the Penman-Monteith evaporation model for surface evaporation (Figure 3.1).

3.1.1 Modelling variably saturated flow

The Richards equation (Richards, 1931) will be used to model infiltration and variably saturated flow in the soil. This is a non-linear partial differential equation that combines the Darcy-Buckingham equation and the continuity equation (formulated here for one dimension):

$$\frac{\partial \theta(h)}{\partial t} = \frac{\partial}{\partial z}\left(K(h)\frac{\partial h}{\partial z}\right) + \frac{\partial K(h)}{\partial z} - S(h) \tag{3.1}$$

where θ is the volumetric water content $[-]$, t is time $[T]$, z is a spatial coordinate $[L]$, $K(h)$ is the hydraulic conductivity as a function of the pressure head $\left[LT^{-1}\right]$, and $S(h)$ is a sink function representing the water uptake by roots. The formulation above is the mixed form of the Richards equation, referring to the presence of two dependent variables: θ and h, where the rate of change in water content is expressed by the sum of the capillary flow term and gravity flow term minus a sink term.

When $\frac{d\theta}{dt}$ is represented by a soil water capacity function $C_w(h)$ that characterises the slope of the retention curve, the Richards equation can also be expressed in terms of pressure head only. This way, we obtain the pressure head formulation:

$$C_w(h)\frac{\partial}{\partial t} = \frac{\partial}{\partial z}\left(K(h)\frac{\partial}{\partial z}\right) + \frac{\partial K(h)}{\partial z} - S(h) \tag{3.2}$$

In HYDRUS we use numerical methods to solve the Richards equation: the finite element numerical approach is used in space and the finite difference approach is used in time.

$C_w(h)$ can be found using the Van Genuchten soil water retention function, which is formulated as (Van Genuchten, 1980):

$$S_e(h) = \frac{1}{[1 + (-\alpha h)^n]^m} \tag{3.3}$$

where S_e is the effective soil water saturation and α [−], n [−], and m [−] are fitting parameters. Given that effective soil water saturation is also given by:

$$S_e = \frac{\theta - \theta_r}{\theta_s - \theta_r} \tag{3.4}$$

where θ_r is the residual water content and θ_s is the saturated water content. When substituting S_e in Equation 3.4 with Equation 3.3 and solving for $\theta(h)$ we obtain:

$$\theta(h) = \frac{\theta_s - \theta_r}{[1 + (-\alpha h)^n]^m} + \theta_r \tag{3.5}$$

Subsequently, the soil water capacity function $C_w(h)$ is defined as:

$$C_w(h) = \frac{d\theta}{dh} = \frac{\alpha^n(\theta_s - \theta_r)mn(-h)^{n-1}}{[1 + (-\alpha h)^n]^{m+1}} \tag{3.6}$$

3.1.2 Modelling root uptake (based on Feddes et al., 2001; Šimůnek et al., 2009)

The maximum possible (i.e. potential) water extraction rate by plants $S_p(z)$ $\left[T^{-1}\right]$ under optimal soil moisture conditions, integrated over the rooting depth D_{root}, equals the potential transpiration rate T_p $\left[LT^{-1}\right]$ (Feddes et al., 2001). S_p for a given depth z is then given by the fraction of the root length density at depth z over the total root length density for the entire rooting depth D_{root}:

$$S_p(z) = \frac{\pi_{root}(z)}{\int_{-D_{root}}^{0} \pi_{root}(z)\partial z} T_p \tag{3.7}$$

$$potential\,root\,water\,uptake\,rate = \frac{root\,length\,density}{total\,root\,length\,density} \times potential\,transpiration\,rate$$

The influence of water and salinity stress on water extraction by roots may be expressed by multiplication factors, yielding:

$$S(z) = \alpha_{rw}\alpha_{rs}S_p(z) \tag{3.8}$$

where $S(z)$ is the actual water flux density at depth z, and α_{rw} and α_{rs} are reduction factors related to water and salinity stress, respectively. Assuming that salinity stress may be neglected for the study area, equation 3.8 can be reduced to:

$$S(z) = \alpha_{rw}S_p(z) \tag{3.9}$$

The above equations relate to water extraction as a function of a specific root depth, and since root growth and thus rooting depth depend on the pressure head at which water is available, we model root uptake by defining the sink term S as follows (Feddes et al., 1974):

$$S(h) = \alpha(h)S_p \tag{3.10}$$

where $S(h)$ is the volume of water removed from a unit of soil per unit of time as a result of water uptake by plants, $\alpha(h) = \alpha_{rw}(h)$ is a dimensionless water stress response function for root uptake ($0 \leq \alpha \leq 1$) and S_p is the potential root uptake rate.

The purpose of the root uptake model is first to simulate water extraction by the trees on either side of the cropping row over the course of the period of several hours during and following a rainfall episode. In a second approach we want to account for the different vegetation types and vegetation units (tree, crop) that are found along the simulated transect perpendicular to the alley.

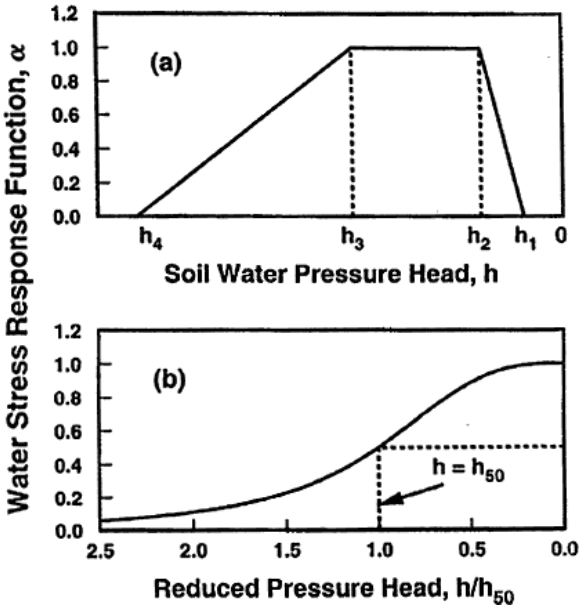

Figure 3.2: The water stress response function $\alpha(h)$ as defined by: (a) Feddes et al. (1978) and (b) Van Genuchten (1987). Original diagrams redrawn by Šimůnek et al. (2009).

The following sections continue with a detailed discussion of the various stress response functions that are at our disposal. For the sake of parameterisation and parsimony, we will use the linear water stress response function (Feddes et al., 1978) with a root distribution that does not change over time (Vrugt et al., 2001a). We will at this time not account for solute transport or osmotic stress, nevertheless we have included a description of a nonlinear water and osmotic stress response function (Van Genuchten, 1987) in combination with time-variable rooting depth (Verhulst, 1838; Pearl and Reed, 1920).

3.1.2.1 Linear water stress response function (Feddes et al.)

The water stress response function α can be defined in multiple ways as shown in Figure 3.2. Feddes et al. (1978) approximated water stress by a continuous linear function defined by four pressure head values, which they numbered h_1 to h_4. Water uptake is assumed zero for pressure heads higher than the field capacity h_1 ($pF \approx 2$ for sand, $pF \approx 2.4$ for silt and $pF \approx 2.5$ for clay), also called the anaeobiosis point, and for pressure heads lower than wilting point h_4 ($pF \approx 4.2$ for sand, silt and clay). Between h_2 and h_3 the water uptake rate equals S_p (see Equation 3.10) when water stress is minimal, in which case $\alpha(h) = 1$.

3.1.2.2 Nonlinear water and osmotic stress response function (Van Genuchten, 1987) and root distribution (Vrugt et al., 2001a,b)

The water stress response function formulated by Van Genuchten (1987) is an adapted version of Feddes et al. (1978) and in addition accounts for osmotic stress, which is the stress caused by the presence of solutes:

$$S(h, h_\phi) = \alpha(h, h_\phi) S_p \tag{3.11}$$

where $h_\phi$is the osmotic head given by:

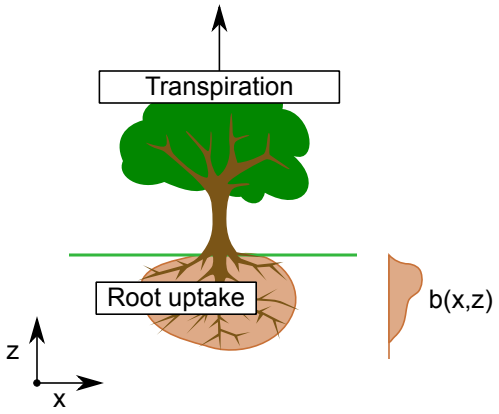

Figure 3.3: Two-dimensional distribution of potential water uptake defined by Vrugt et al. (2001a,b).

$$h_\phi = a_i c_i \tag{3.12}$$

where c_i is a linear combination of i solutes and a_i are the corresponding experimental coefficients that define the relationships between solute concentration and osmotic head for a particular solute. The influence of the osmotic head on the reduction of root uptake can be considered as either additive:

$$\alpha(h, h_\phi) = \frac{1}{1 + \left(\frac{h+h_\phi}{h_{50}}\right)^p} \tag{3.13}$$

Or multiplicative:

$$\alpha(h, h_\phi) = \frac{1}{1 + \left(\frac{h+h_\phi}{h_{50}}\right)^{p_1}} \frac{1}{1 + \left(\frac{h+h_\phi}{h_{\phi 50}}\right)^{p_2}} \tag{3.14}$$

where p, p_1 and p_2 are experimental constants corresponding to the solute. h_{50} now is the pressure head at which the root uptake rate $S(h)$ is reduced to 50% under negligible osmotic stress conditions ($\alpha(h_\phi) = 1$). Conversely, $h_{\phi 50}$ is the osmotic head at which the root uptake rate $S(h)$ is reduced to 50% under neglegible water stress conditions ($\alpha(h) = 1$). Figure 3.2b shows the S-shaped water uptake stress response function defined by Van Genuchten (1987). The curve is much smoother than the function defined by Feddes et al. (1978), however it does not account for the reduction in root uptake for pressure heads exceeding the field capacity, including saturated conditions. This is however not a problem for simulations where the duration of saturated conditions is relatively short compared to total duration of the period where pressure head is between wilting point and field capacity.

The root growth model discussed in the previous section can be replaced by a time-invariant root distribution, in which case the dimensionless shape factor describing the two-dimensional distribution of potential water uptake becomes (Vrugt et al., 2001b,a):

$$b(x, z) = \left(1 - \frac{z}{Z_m}\right)\left(1 - \frac{x}{X_m}\right) e^{-\left(\frac{p_z}{Z_m}|z^* - z| + \frac{p_r}{X_m}|x^* - x|\right)} \tag{3.15}$$

where $b(x, z)$ is the potential water uptake distribution function, where X_m and Z_m are the maximum rooting length and maximum rooting depth, respectively, x and z are distances from the origin of the plant or tree at the surface, p_x, x^*, p_z and z^* are empirical parameters used to

ensure zero water uptake at $z = Z_m$. In HYDRUS, x^* and $z^*$are called the radius and depth of maximum intensity, respectively. The potential water uptake can now be calculated for a root zone with arbitrary shape (Vogel, 1987):

$$S_p = b(x, z)S_t T_p \tag{3.16}$$

where T_p is the potential transpiration rate and S_t is the diameter of the zone through which the plant transpires.

In short, rather than simulating the physical presence of a distributed root system, the potential water uptake is simulated by a potential water uptake distribution function. Following this approach, it is equally possible to represent a variety of different root systems of different vegetation with one potential water uptake distribution function.

3.1.2.3 Nonlinear water and osmotic stress response function (Van Genuchten, 1987) in combination with time-variable rooting depth (Verhulst-Pearl)

We have discussed two root uptake models that can be used within the HYDRUS software package, one that uses a simple water stress response function $\alpha(h)$ (Feddes et al., 1978) and another that uses a water stress response function $\alpha(h, h_\phi)$ and which also accounts for osmotic stress caused by solutes (Van Genuchten, 1987). HYDRUS also offers the possibility to use a model that accounts for time-variable rooting depth (Hoffman and Van Genuchten, 1983; Šimůnek and Suarez, 1993), in which case the actual water uptake distribution is given by the generalised function:

$$S(h, h_\phi, x) = \alpha(h, h_\phi, x)b(x)T_p \tag{3.17}$$

where $x = 0$ represents the bottom of the soil profile (lower boundary of the domain), and $b(x)$ is a function that describes the normalised water uptake distribution, which may be constant with depth, linear (as explained above; Feddes et al., 1978), or (Hoffman and Van Genuchten, 1983):

$$b(x) \begin{cases} \frac{1.66667}{L_R} & x > L - 0.2L_R \\ \frac{2.0833}{L_R}\left(1 - \frac{x_0 - x}{L_R}\right) & x \in (L - L_R; L - 0.2L_R) \\ 0 & x < L - L_R \end{cases} \tag{3.18}$$

where L is the depth of the soil profile with respect to $x = 0$ $[L]$, L_R is the root depth $[L]$. The water uptake distribution $b(x)$ can be modified in HYDRUS by modifying the parameters of Equation 3.18, on the condition that $b(x)$ is a continuous function.

The integration of the actual water uptake function (Equation 3.17) gives the actual transpiration rate T_a:

$$T_a = \int_{L_R} S(h, h_\phi, x)dx = T_p \int_{L_R} a(h, h_\phi, x)b(x)dx \tag{3.19}$$

Root depth L_R can be constant or variable. In the case where root depth is variable during the simulation, HYDRUS calculates the actual root depth as:

$$L_R(t) = L_m f_r(t) \tag{3.20}$$

where L_m is the maximum rooting depth and $f_r(t)$ is the root growth coefficient defined by the Verhulst-Pearl logistic growth function (Verhulst, 1838; Pearl and Reed, 1920):

$$f_r(t) = \frac{L_0}{L_0 + (L_m - L_0)e^{-rt}} \tag{3.21}$$

where L_0 is the initial root depth and r is the growth rate.

3.1.3 Modelling evapotranspiration (Šimůnek et al., 2009)

Evapotranspiration is modelled using the Penman-Monteith equation, which defines the actual transpiration rate ET_0 $[LT^{-1}]$ as a radation term ET_{rad} added to the aerodynamic term ET_{aero}. (Penman, 1948; Monteith, 1981; Monteith and Unsworth, 1990; FAO, 1990):

$$ET_0 = ET_{rad} + ET_{aero} = \frac{1}{\lambda}\left[\frac{\triangle\,(R_n - G)}{\triangle + \gamma\,(1 + r_c/r_a)} + \frac{\rho_a c_p (e_s - e_a)/r_a}{\triangle + \gamma\,(1 + r_c/r_a)}\right] \tag{3.22}$$

where λ is the latent heat of vaporisation $\left[MJ\,kg^{-1}\right]$, R_n is the net radiation at the soil surface $\left[MJ\,m^{-2}d^{-1}\right]$, G is the heat transfer into the soil $\left[MJ\,m^{-2}d^{-1}\right]$, ρ is the atmospheric density $\left[kg\,m^{-3}\right]$, c_p is the specific heat of moist air $[1.013\,kJ\,kg^{-1\circ}C^{-1}]$, $(e_s - e_a)$ is the vapor pressure deficit $[kPa]$ between the saturation vapor pressure e_s at temperature T and the actual vapor pressure e_a, r_c is the crop canopy resistance $[sm^{-1}]$ and r_a is the aerodynamic resistance $[sm^{-1}]$. The heat transfer G into the soil is relatively small, and may therefore be neglected.

3.2 Model domain and parameterisation

This section continues with a description of the HYDRUS model domain and parameters. The parameter descriptions were taken from the HYDRUS 2D/3D User Manual (Šejna et al., 2011).

3.2.1 Model geometry

A two-dimensional system is defined that represents a vertical transect of the alley cropping system in the plane perpendicular to the tree rows (Figure 3.4). The following parameters are used to define the system:

- Total depth of the soil profile z
- Total width of the soil profile x
- Number of soil materials and spatial configuration of these materials

3.2.2 Boundary conditions

Upper boundary condition The pressure head applied to the upper boundary of the system is variable in time as a result of time-variable rainfall

Lower boundary condition The lower boundary of the system is set to free drainage, meaning the variable flux is determined as $q(n) = -K(h)$, where h is the local pressure head and $K(h)$ the corresponding hydraulic conductivity

Lateral boundary conditions Lateral boundaries are set to no flow, since lateral flow in the upper soil layers is assumed zero due to the low gradient and the relatively long distance to the tree rows.

3.2.3 Time discretisation

Time steps have a constant duration, where the time discretisation is defined by the parameters:

t_0 Initial time

t_i Final time

Δt Time step duration

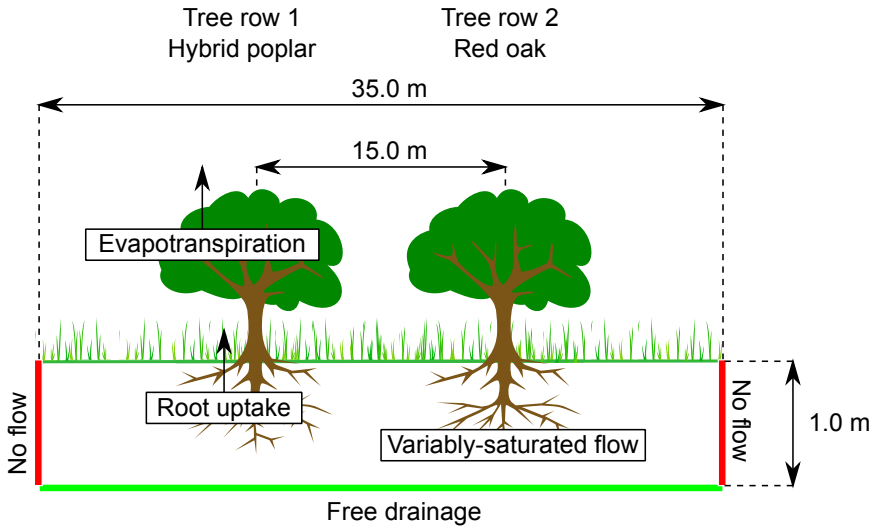

Figure 3.4: Geometry and boundary conditions and simuled processes (not to scale).

3.2.4 Water flow parameters

θ_r Residual water content

θ_s Saturated water content

α Fitting parameter in the soil water retention function

n Fitting parameter in the soil water retention function

m Fitting parameter in the soil water retention function

K_s Hydraulic conductivity at saturation

3.2.5 Root uptake parameters (Šejna et al., 2011)

3.2.5.1 Feddes root uptake model

The following parameters are used for the water stress response function illustrated in Figure 3.2 on page 33.

$P0$ h_1 in Figure 3.2. Pressure head below which roots start extracting water from the soil, which is the *air-entry suction* or anaerobiosis point. Value fixed at $h = -10\,cm$ ($pF = 1$) for sandy soils.

P_{opt} h_2 in Figure 3.2. Pressure head below which roots start extracting water at the maximum possible rate, also called *field capacity*. This condition of optimal water uptake exists between pressure heads P_{opt} and $P2$. Value fixed at $h = -100\,cm$ ($pF = 2$) for sandy soils.

$P2H$ h_3 in Figure 3.2. Value of the limiting pressure head below which roots can no longer extract water at the maximum rate. Between $P2$ and $P3$ water uptake decreases linearly with pressure head.

$P2L$ As $P2L$, but for a potential transpiration rate of $r2L$.

$P3$ h_4 in Figure 3.2. Pressure head below which water uptake ceases, usually the *wilting point*. Value fixed at $h = -15000\,cm$ ($pF = 4.2$) for sandy soils.

$r2H$ Potential transpiration rate.

3.2.5.2 Root distribution

Empirical parameters of the dimensionless shape factor, which describes the two-dimensional distribution of potential water uptake. These parameters are introduced to ensure zero water uptake at the outer edges of the root system (where $x = X_m$ and $z = Z_m$):

x^* Radius of maximum intensity; value based on field data provided by Alain Cogliastro.

z^* Depth of maximum intensity; value based on field data provided by Alain Cogliastro.

p_x Empirical parameter; value fixed at $p_x = 1$

p_z Empirical parameter; value fixed at $p_z = 1$

3.2.6 Evapotranspiration parameters (Šejna et al., 2011)

λ Latent heat of vaporisation

R_n Net radiation at the soil surface

G Heat transfer into the soil (assumed zero)

ρ Atmospheric density

$(e_s - e_a)$ Vapor pressure deficit

Chapter 4

Recommendations

4.1 Field study

Regarding the field site, equipment, and measurements:

- Reduce humidity inside the Hobo U30 monitoring systems (known issue) by sealing the housing with duct tape.
- FDR setup: Measure exact altitude of each FDR sensor location in the field with an automatic level. This method allows for the detection of irregularities in the relief.
- FDR setup: Power problems due to insufficient solar energy have lead to early termination of measurement for many FDR sensors (see Figure 2.14 on page 26). Instead of using the 10 Ah batteries that can be placed inside the Hobo U30 weatherproof housing, we recommend the use of 12 V deep cycle batteries (not regular car batteries) that have a lifespan of several years of outdoor operation and resist relatively well to temperature changes. For optimal protection place in a white-coloured box and seal with duct tape. Estimated cost: $200 per battery, total $600.
- FDR setup: Issues with at least three sensors: 9938710, 9925296, 9925307. These sensors did not work at some point during the measurement period and must be tested together with the extension cables that connect them to the monitoring system. We have one spare FDR sensor, so it might be necessary to buy 3-4 new FDR sensors type Onset S-SMD-M005, estimated cost between $477-$700
- Record the exact coordinates of all devices used in the field experiments using a GPS receiver.
- Weather monitoring: The weather station was unmounted and brought back to the INRS-ETE in Quebec. We plan on remounting the weather station on the same location at St. Paulin in the early spring of 2012 (April).
- Soil mapping: We noticed that the perched, (nearly) saturated water table is not found at the same depth for all FDR sensor sets. Modelling could be helped by obtaining additional data on soil texture using simple soil core sampling equipment (hand auger including a T-shaped handle, one or two 3' sections of shaft and an auger tip). Since the terrain slopes in two direction, we can take 12 soil core samples in two rows, one row parallel to the alley and one perpendicular to the alley. Estimated duration of this experiment is one day. Costs depend on whether or not we can borrow the hand auger.

- Field site: It is possibile to extend the experiment to other field sites e.g. in Montérégie or the research site of the agroforestry department of the University of Guelph. Such decision must count on the support of the other contributors to PACC-26, and since no contributor has proposed to extend the experiment to other sites we will continue to concentrate on the St. Paulin alley cropping system during the 2012 field work season.

4.2 Modelling

The PAR sensor monitors the electromagnetic spectrum between 400-700 nm. This range is not large enough to estimate evaporation from the soil surface, and the ideal case we would have needed a pyranometer (range 300-1100 nm, Onset S-LIB-M003 with an estimated price of $210 ex vat). We now have to figure out a way to translate PAR sensor data into net radiation at the soil surface, which is parameter R_n in the Penman-Monteith evapotranspiration model.

Bibliography

American National Standard Institute, 1972. Standard method of particle-size analysis of soils. Designation D 422–63, pp. 69–79. American National Standard A37.145.1972.

Bambrick, A. D., Whalen, J. K., Bradley, R. L., Cogliastro, A., Gordon, A. M., Olivier, A., Thevathasan, N. V., 2010. Spatial heterogeneity of soil organic carbon in tree-based intercropping systems in Quebec and Ontario, Canada. Agroforestry Systems 79, 343–353.

Caya, D., Laprise, R., 1999. A semi-implicit semi-lagrangian regional climate model: The Canadian RCM. Monthly Weather Review 3, 341–362.

Comité Canadien de Pédologie, 1978. Manuel de méthodes d'échantillonage et d'analyse des sols. Agriculture Canada, Ottawa, Canada, 4–32.

FAO, 1990. Expert consultation on revision of FAO methodologies for crop water requirements. Food and Agriculture Organization of the United Nations. World Soil Resources Reports, Ch. Annex V: FAO Penman-Monteith Formula.

Feddes, R. A., Bresler, E., Neuman, S. P., 1974. Field test of a modified numerical model for water uptake by root systems. Water Resources Research 10 (6), 1199–1206.

Feddes, R. A., Hoff, H., Bruen, M., Dawson, T., De Rosnay, P., Dirmeyer, P., Jackson, R. B., Kabat, P., Kleidon, A., Lilly, A., Pitman, A. J., 2001. Modeling root water uptake in hydrological and climate models. Bulletin of the American Meteorological Society 82 (12), 2797–2809.

Feddes, R. A., Kowalik, P. J., Zaradny, H., 1978. Simulation of Field Water Use and Crop Yield. John Wiley & Sons, New York, NY.

Garrett, G., Walter, W., Godsey, L. D., 2011. Alley cropping: a relic from the past or a bridge to the future. Inside Agroforestry 19 (2), 1–11.

Gumiere, S. J., Le Bissonnais, Y., Raclot, D., Cheviron, B., 2010a. Vegetated filter effects on sedimentological connectivity of agricultural catchments in erosion modelling: a review. Earth Surface Processes and Landforms.

Gumiere, S. J., Raclot, D., Cheviron, B., Davy, G., Louchart, X., Fabre, J.-C., Moussa, R., Le Bissonnais, Y., 2010b. MHYDAS-Erosion: A distributed single-storm water erosion model for agricultural catchments. Hydrological Processes.

Gumiere, S. J., Rousseau, A. N., 2011. Development of VFDM: A riparian vegetated filter dimensioning model. In: International Symposium on Erosion and Landscape Evolution, American Society of Agricultural and Biological Engineers, Anchorage, AK, 18 September, 2011.

Hoffman, G. J., Van Genuchten, M. T., 1983. Limitations and Efficient Water Use in Crop Production. Am. Soc. Of Agron., Madison, WI, Ch. Soil properties and efficient water use: Water management for salinity control, pp. 73–85.

Mailhot, A., Duchesne, S., Caya, D., Talbot, G., 2007. Assessment of future change in intensity-duration-frequency (IDF) curves for Southern Quebec using the Canadian Regional Climate Model (CRCM). Journal of Hydrology 347, 197–210.

Monteith, J., Unsworth, M., 1990. Principles of Environmental Physics. Edward Arnold, London.

Monteith, J. L., 1981. Evaporation and surface temperature. Quarterly Journal of the Royal Meteorological Society 107, 1–27.

Mpelasoka, F. S., Chiew, F. H. S., 2009. Influence of rainfall scenario contruction methods on runoff projections. Journal of Hydrometeorology 10, 1168–1183.

Murphy, J., Sexton, D., Jenkins, G., Boorman, P., Booth, B., Brown, C., Clark, R., Collins, M., Harris, G., Kendon, E., Betts, R., Brown, S., Howard, T. P., Humphrey, K. A., McCarthy, M. P., McDonald, R. E., Stephens, A., Wallace, C., Warren, R., Wilby, R., Wood, R. A., 2009. UK Climate Projections Science Report: Climate change projections. Met Office Hadley Centre, Exeter.

Music, B., Caya, D., 2007. Evaluation of the hydrological cycle over the Mississippi River basin as simulated by the Canadian Regional Climate Model (CRCM). Journal of Hydrometeorology 8, 969–988.

Pearl, R., Reed, L., 1920. On the rate of growth of the population of united states since 1790 and its mathematical representation. Proceedings of the National Academy of Sciences USA G 6 (6), 275.

Penman, H. L., 1948. Natural evaporation from open water, bare soil and grass. Proceedings of the Royal Society A 193 (1032), 120–145.

Plamboeck, A. H., Grip, H., Nygren, U., 1999. A hydrological tracer study of water uptake depth in a Scots pine forest under two different water regimes. Oecologia 119, 452–460.

Richards, L. A., 1931. Capillary conduction of liquids through porous mediums. Physics 1, 318–333.

Van Genuchten, M. T., 1980. A closed-form equation for predicting the hydraulic conductivity of unsaturated soils. Soil Science Society of America Journal 44, 892–898.

Van Genuchten, M. T., 1987. A numerical model for water and solute movement in and below the root zone. Research Report No 121. U.S. Salinity Laboratory, USDA, ARS, Riverside, California.

Verhulst, P., 1838. Notice sur la loi que la population suit dans son accroissement. Curr. Math. Phys. 10, 113.

Vogel, T., 1987. SWMII – Numerical model of two-dimensional flow in variably saturated porous medium. Research report 87, Department of Hydraulics and Catchment Hydrology, Wageningen University, The Netherlands.

Vrugt, J. A., Hopmans, J. W., Šimůnek, J., 2001a. Calibration of a two-dimensional root water uptake model. Soil Science Society of America Journal 65 (4), 1027–1037.

Vrugt, J. A., Van Wijk, M. T., Hopmans, J. W., Šimůnek, J., 2001b. One-, two-. and three-dimensional root water uptake functions for transient modeling. Water Resources Research 37 (10), 2457–2470.

Šejna, M., Šimůnek, J., Van Genuchten, M. T., 2011. The HYDRUS software package for simulating two- and three-dimensional movement of water, heat and multiple solutes in variably-saturated media. User manual, version 2.0. PC Progress, Prague, Czech Republic.

Šimůnek, J., Suarez, D. L., 1993. The SOILCO2 code for simulating one-dimensional carbon dioxide production and transport in variably saturated porous media. Version 1.1, Research Report No. 127. Major ion chemistry model for variably saturated porous media. U.S. Salinity Laboratory, USDA, ARS, Riverside, California.

Šimůnek, J., Van Genuchten, M. T., Šejna, M., 2011. The HYDRUS software package for simulating two- and three-dimensional movement of water, heat and multiple solutes in variably-saturated media. Technical manual, version 2.0. PC Progress, Prague, Czech Republic.

Šimůnek, J., Vogel, T., Van Genuchten, M. T., 1992. The SWMS_2D code for simulating water flow and solute transport in two-dimensional variably saturated media, version 1.1. Research report 126, U.S. Salinity Laboratory, USDA, ARS, Riverside, CA.

Šimůnek, J., Šejna, H., Saito, H., Sakai, M., Van Genuchten, M. T., 2009. The HYDRUS-1D software package for simulating the one-dimensional movement of water, heat, and multiple solutes in variably-saturated media. Version 4.08. University of California Riverside, Department of Environmental Sciences, Riverside, California.

Wilson, N. R., Shaw, R. H., 1977. A higher order closure model for canopy flow. Journal of Applied Meteorology 16 (11), 1197–1205.

List of Tables

List of Figures